

Shot Noise in Helical Edge States in Presence of a Static Magnetic Defect

R. A. Niyazov^{a,b,*}, I. V. Krainov^b, D. N. Aristov^{a,b,c}, and V. Yu. Kachorovskii^b

^a Petersburg Nuclear Physics Institute, National Research Center Kurchatov Institute, Gatchina, 188300 Russia

^b Ioffe Institute, St. Petersburg, 194021 Russia

^c Faculty of Physics, St. Petersburg State University, St. Petersburg, 199034 Russia

*e-mail: niyazov_ra@pnpi.nrcki.ru

Received December 28, 2023; revised January 23, 2024; accepted January 24, 2024

The Fano factor, \mathcal{F} , of the shot noise of the current through the edge states of a two-dimensional topological insulator with contacts of generic type is calculated. A magnetic static defect changes \mathcal{F} significantly. For metallic contacts, as the strength of the defect increases, the Fano factor increases from $\mathcal{F} = 0$ to its maximum value, $\mathcal{F}_{\max} \approx 0.17$, and then decreases back to zero value in the limit of strong defect. For tunnel contacts in the limit of weak tunnel coupling, the Fano factor is insensitive to the strength of the defect: $\mathcal{F} \rightarrow 1/2$. For weak but finite tunnel coupling strength, \mathcal{F} exhibits a periodic series of sharp peaks of small amplitude as a function of the magnetic flux piercing the sample. The peaks transform into Aharonov–Bohm harmonic oscillations with increasing the strength of the tunnel coupling.

DOI: 10.1134/S0021364024600186

1. INTRODUCTION

The study of electrical and optical properties of the topological insulators (TI), i.e., materials that are insulators in the bulk, but have conducting states at the boundary [1–3], is one of the hot topics actively discussed in the last decade. In particular, in two-dimensional (2D) TI, non-trivial topology of bulk bands leads to the appearance of helical one-dimensional (1D) states which conduct the current along the edges of the sample without dissipation. The propagation of electrons in such 1D channels is characterized by a certain helicity, i.e., electrons with opposite spins traveling in opposite directions. A remarkable consequence of this feature is the prohibition of backscattering by non-magnetic impurities, and precisely due to this property there is no dissipation in such channels.

The best known implementation of 2D TI are the quantum wells in HgTe/CdTe-based structures, the topological properties of which were predicted theoretically [4, 5] and confirmed by a series of experiments, including measurements of the conductance of edge states [6] and experimental evidence of nonlocal transport [7–10].

If one attaches two non-magnetic contacts to an edge of a 2D TI and shift (for example, by using a gate) the Fermi level into the band gap, then the conductance of such a device will be completely determined by the properties of the edge states (see Fig. 1). Since the sample boundary can be bypassed in two direc-

tions, such a system is an interferometer. Accordingly, both the average current and its noise depend on interference effects and, as a consequence, the observed quantities in such systems can be controlled due to the Aharonov–Bohm (AB) effect [11–17]: they periodically depend on the magnetic flux penetrating the region encompassed by electronic states.

Typically, interference is suppressed when T becomes larger than the distance, Δ , between levels of the system. As was recently shown theoretically [14–17], for AB interferometers based on helical edge states (HES), this is not the case, and the interference effects “survive” even in the case $T \gg \Delta = 2\pi v_F/L$ where $L = L_1 + L_2$, $L_{1,2}$ are the lengths of the interferometer arms, and v_F is the Fermi velocity. For typical v_F of order of 10^7 cm/s and typical system sizes (>1 micron), the value of Δ does not exceed a few Kelvin. This means that the interference effects in systems based on HES can be studied at relatively high temperatures, which are relevant for various applications.

We recently discussed the conductance of the AB helical interferometers [14–17] and the properties of the tunnel chain of the AB helical rings [18, 19]. Here we will discuss another observable quantity—the current shot noise.

The shot noise in HES has already been discussed many times [20–32]. However, the role of the interference effects in the noise has previously been discussed

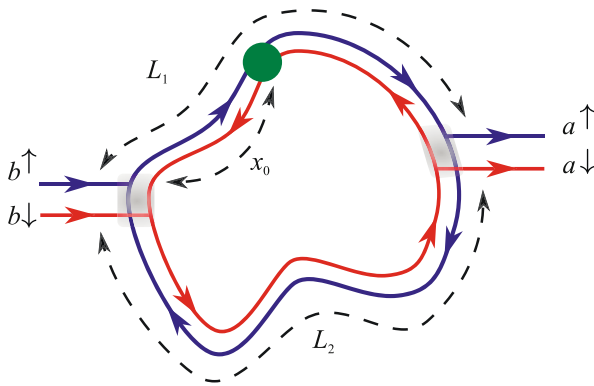


Fig. 1. (Color online) AB helical interferometer. The green dot indicates a MD. Contact areas are highlighted in grey.

only in geometry other than shown in Fig. 1 and in a different regime, $(T, eV) \ll \Delta$, where V is the bias voltage [22, 23]. Usually, an infinite boundary of a TI is considered, in which there is some kind of defect leading to backscattering, for example, a dynamic magnetic impurity. Actually, spin-unpolarized electrons entering the HES through a non-magnetic contact (tunnel or metal) have equal probabilities to jump into the right-moving state with a certain spin and to the left-moving one with the opposite spin (see below the expression (7) for the scattering matrix of a non-magnetic contact). Therefore, for a finite size sample in standard two-terminal geometry (see Fig. 1), the electron can reach the second contact and exit the sample moving clockwise or counterclockwise. Moreover, for any contacts, with the exception of purely metallic ones (for example, for tunnel contacts or quantum point contacts), there is a finite probability of passing by the contact without leaving the sample, i.e., both “right-handed” and “left-handed” electrons can wind around the sample several times before coming out to the contact, and the corresponding processes can interfere. Note that quantum point contacts to the HES have already been realized experimentally [33], so that possible manifestations of interference effects in conductance and noise allow experimental verification, especially having in mind that condition $T \gg \Delta$ does not require very strict restrictions on temperature.

At the same time, in contrast to the standard AB interferometer based on conventional (non-helical) states, in a helical interferometer the right and left electronic states have opposite spins at each point and, as a consequence, there is no interference at ballistic case. Interference contributions to the conductance and the noise appear in the presence of backscattering in one of the interferometer arms. Such scattering can be caused, for example, by a MD or a charged island tunnel-coupled to the HES. It is worth noting that interference effects in a helical interferometer are not reduced to AB oscillations (examples of interference

processes independent of the magnetic field are given in [16], see Section 4).

The problem of the dynamic magnetic impurity in the HES has been studied in great detail (see, for example, works [25, 28–32]). The main idea was to take into account the back action of electrons in the infinite HES on a magnetic impurity, whose magnetic moment changes direction after each scattering event. Then, for an isotropic exchange interaction between the impurity and the HES, the magnetic moment of the impurity relaxes after some time (the so-called Korringa time) towards the direction of the electron spin in the HES at the point where the impurity is located and, as a consequence, the interaction between the impurity and the HES completely “switches off” (see discussion in [25]). Accordingly, the problem of the noise intensity at zero frequency in the HES with a single impurity makes sense only in the presence of an anisotropic exchange interaction [28] (or an external magnetic field acting on a dynamic impurity, see discussion in [32]). This can be seen, for example, from the final formulas for the Fano factor (FF), obtained in the work [28]. These formulas are singular in the limit of isotropic exchange ($p = 1, q = 1$ in the notation [28]), i.e., the result for the FF depends on the order in which the constants responsible for the anisotropy tend to zero (see also discussion in [27]).

In this sense, measuring the FF in an experiment according to the problem setup in [28] will provide more information about the properties of the impurity (for example, about the anisotropic exchange constants) than properly about the HES. At the same time, in a real situation, the relaxation of the magnetic moment of the impurity is caused not only by the interaction with the HES, but also with the environment of the impurity, which will immediately give a non-singular response for the FF in case of the isotropic exchange interaction. Therefore, it seems no less interesting to study the case that is completely opposite to the case considered in the papers [25, 28–32], namely, the case of a static MD with a large spin, which is robustly connected to the external environment. In this formulation, the influence of the HES on the magnetic moment of the defect can be neglected. This is precisely the case which we will consider in this work.

Specifically, we assume that there is a potential dielectric ferromagnetic contact (magnetic needle) with high magnetic stiffness. The direction of the magnetic moment of the defect is determined by the exchange anisotropy inside the dielectric and by the demagnetization tensor. Such a defect ensures the existence of a magnetic field in a small region of the HES, i.e., allows elastic backward scattering without tunneling coupling between the HES and defect. Note that the possibility of creating static magnetic contacts to the HES has already been discussed in another context [34]. In principle, the interference

effects we are interested in could be observed in presence of a point-like non-magnetic scatterer, taking into account the electron–electron interaction [35]. In the latter case, however, an analysis of inelastic effects is required, which is beyond the scope of this work.

For one spinless quantum channel, the shot noise intensity is proportional to the product of the transmission \mathcal{T} and the reflection $\mathcal{R} = 1 - \mathcal{T}$ coefficients of the scatterer:

$$S(\omega = 0) \propto \mathcal{T}(1 - \mathcal{T}).$$

A convenient measure of shot noise is the FF, $\mathcal{F} = S(\omega = 0)/2eI$, where I is the current in the channel.

Experimental measurement of the FF at zero magnetic field for the edge states of 2D TI gives the value $0.1 < \mathcal{F} < 0.3$ [24, 26]. The upper value 0.3, is close to the $1/3$ value for diffusive conductor. A similar answer is obtained in the model of a large number of “islands,” tunnel-connected to the HES, in which the spin can relax [36]. The effect of such islands on HES is currently being actively debated (see [37] and references therein).

In this work, we study the shot noise FF for the current flowing through the edge states of the 2D TI to which two identical contacts are connected, which can be of metal or tunnel character. A fixed bias voltage V is applied to the contacts. We will consider the most interesting and easily realized case:

$$\Delta \ll T \ll eV. \quad (1)$$

For simplicity, we model the external system with a conventional (non-helical) single-channel wire with spin and describe the junction of the interferometer with the external system by real amplitudes t , r ($t^2 + r^2 = 1$), where r is the amplitude of the tunneling from the external contact to the edge state of the sample, and t is the amplitude of the passage along the HES passing the contact (without exiting the sample) (see Fig. 2). Although this model of the contact is very simplified, it is commonly used in the quantum interferometry, starting from the work [38], since it allows one to describe the transition from the metal contact ($t = 0$) to the tunnel contact ($t = 1$). In particular, this model qualitatively describes quantum point contacts to the HES, which have already been used in the recent experiment [33].

We assume that there is a static MD at the edge of the system. The goal of the work is to calculate $\mathcal{F}(t, \theta, \phi)$, where θ describes the scattering strength on the MD ($\theta = 0$ is the absence of the defect, $\theta = \pi/2$ is a strong, ideally reflective defect), and $\phi = \Phi/\Phi_0$, where Φ is the magnetic flux through the sample, and Φ_0 is the flux quantum. As we will show, for metal contacts FF does not depend on ϕ , and the MD strongly *enhances* the FF. There is an optimal value of the defect strength $\theta_{\max} \approx 0.28\pi$, which gives the max-

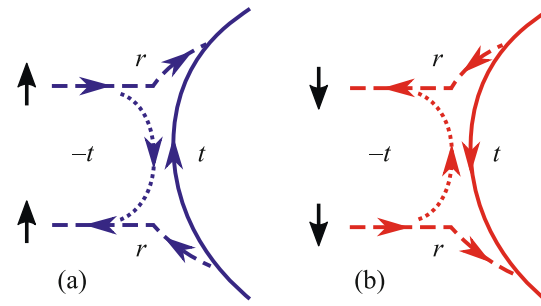


Fig. 2. (Color online) The scattering amplitudes of contacts, which for simplicity are modeled as a single-channel wire with the spin. It is assumed that there is no spin flip at the contact so that two spin polarizations at the contact are completely separated. The $t \rightarrow 1$ case corresponds to a tunnel contact, and the $t \rightarrow 0$ case models a metal contact.

imum value of the FF, $\mathcal{F}_{\max} \approx 0.17$. On the contrary, for tunnel contacts, FF is insensitive to both the flux and the strength of the defect and is equal to $\mathcal{F}(1, \theta, \phi) = 1/2$. Moreover, for contacts with the amplitude t close, but not exactly equal 1, MD *reduces* FF. We will also demonstrate that for a contact with an intermediate tunneling amplitude, $0 < t < 1$, the external magnetic field affects the FF, although the total relative change in \mathcal{F} for ϕ changing from zero to one is quite small ($\lesssim 0.1$).

2. FORMULATION OF THE PROBLEM

The current noise is related with fluctuations of the electric current with respect to its average value $\delta\hat{I}(t) = \hat{I}(t) - \langle \hat{I} \rangle$. Here \hat{I} is the current operator (an analytical expression for \hat{I} is given in [39, 40]). The current correlation function associated with the noise is defined by:

$$S(t - t') = \frac{1}{2} \langle \delta\hat{I}(t)\delta\hat{I}(t') + \delta\hat{I}(t')\delta\hat{I}(t) \rangle.$$

The Fourier transform of \mathcal{S} gives an expression for the noise power: $S(\omega) = 2 \int_{-\infty}^{\infty} S(t) \exp(i\omega t) dt$ (the factor 2 in this expression is a matter of convention, see formula (1) in [39] and the comment after Eq. (49) in [40]).

Spin-dependent transport through the two-terminal device is fully characterized by the matrix of transmission amplitudes $\hat{t} = t_{\alpha\beta}$ (here α and β are the spin indices associated with the outgoing and the incoming electrons, respectively) [39, 40]:

$$\mathcal{S}(\omega = 0) = \frac{2e^2}{h} \int_{\mu}^{\mu+eV} d\epsilon \text{Tr}[\hat{\mathcal{T}}(\epsilon)(1 - \hat{\mathcal{T}}(\epsilon))], \quad (2)$$

where matrix

$$\hat{\mathcal{T}}(\epsilon) = \hat{t}(\epsilon)\hat{t}^\dagger(\epsilon), \quad (3)$$

is related to the spin-averaged transmission coefficient, $\bar{\mathcal{T}}(\varepsilon)$, by the equation $\bar{\mathcal{T}}(\varepsilon) = \text{Tr}[\hat{\mathcal{T}}(\varepsilon)]/2$. Averaging this expression over the energy, we obtain an expression for the conductance $G = 2(e^2/h)\langle\bar{\mathcal{T}}(\varepsilon)\rangle_\varepsilon$, and find the current,

$$eI = \frac{e^2}{h} \int_{\mu}^{\mu+eV} d\varepsilon \text{Tr}[\hat{\mathcal{T}}(\varepsilon)], \quad (4)$$

and the FF,

$$\mathcal{F} = \frac{\int_{\mu}^{\mu+eV} d\varepsilon \text{Tr}[\hat{\mathcal{T}}(1-\hat{\mathcal{T}})]}{\int_{\mu}^{\mu+eV} d\varepsilon \text{Tr}[\hat{\mathcal{T}}]}. \quad (5)$$

The transmission amplitudes $t_{\alpha\beta}(\varepsilon)$ vary on an energy scale of the distance between levels $\Delta = 2\pi v/L$. We will focus on the most interesting case, when the conditions (1) are satisfied. Then for the FF we have

$$\mathcal{F} = \frac{\text{Tr}\langle\hat{\mathcal{T}}(1-\hat{\mathcal{T}})\rangle_\varepsilon}{\text{Tr}\langle\hat{\mathcal{T}}\rangle_\varepsilon}, \quad (6)$$

where the averaging is taken over a small temperature window in the vicinity of the Fermi level. In the next section we will formulate a model that will allow us to find \mathcal{F} , using the formula (6).

3. MODEL

We consider 2D TI, assuming that the Fermi level is located in the bulk gap, so that the transport between two contacts connected to the system is completely determined by the HES.

The simplest contact scattering matrix has the form

$$\hat{S}_l = \begin{pmatrix} -t & r & 0 & 0 \\ r & t & 0 & 0 \\ 0 & 0 & -t & r \\ 0 & 0 & r & t \end{pmatrix}, \quad t^2 + r^2 = 1, \quad (7)$$

where two identical blocks are responsible for two spins, and the basis is chosen in accordance with the spin polarization of the helical states at the point of contact (red and blue in Fig. 2).

We will assume that at the edge of the TI there is a MD: for example, a potential dielectric ferromagnetic point contact with high magnetic rigidity and with the fixed magnetic moment, the direction of which is determined by uniaxial anisotropy and the demagnetization tensor of the ferromagnet. We describe scattering on such MD by the scattering matrix

$$\hat{S}_M = \begin{pmatrix} \cos\theta & i \sin\theta e^{i\varphi} \\ i \sin\theta e^{-i\varphi} & \cos\theta \end{pmatrix}, \quad (8)$$

that allows for backward scattering, and neglect the back influence of the HES on the parameters of S_M .

The backward scattering rate, $R_\theta = \sin^2\theta$, is determined by the quantity θ while the phase φ has the meaning of the backward scattering phase on the MD.

The matrix of the transmission amplitudes \hat{t} from one contact to another is determined as follows

$$\begin{pmatrix} a^\uparrow \\ a^\downarrow \end{pmatrix} = \hat{t} \begin{pmatrix} b^\uparrow \\ b^\downarrow \end{pmatrix}, \quad (9)$$

where $(b^\uparrow, b^\downarrow)$ and $(a^\uparrow, a^\downarrow)$ are the amplitudes of incoming (from the left contact) and outgoing (to the right contact) waves, respectively (see Fig. 1). This matrix has been obtained earlier [15]:

$$\hat{t} = \frac{r^2 e^{2\pi i \phi L_1/L}}{t} \begin{pmatrix} e^{ikL_1} & 0 \\ 0 & e^{-ikL_1} \end{pmatrix} \begin{pmatrix} t & 0 \\ 0 & 1 \end{pmatrix} \hat{g} \begin{pmatrix} 1 & 0 \\ 0 & 1/t \end{pmatrix}, \quad (10)$$

$$\hat{g} = \cos\theta \left[\begin{pmatrix} 0 & 0 \\ 0 & -1 \end{pmatrix} + \frac{1}{2} \sum_{\alpha=\pm} \frac{1 + \alpha \hat{H}}{1 - t^2 e^{i(kL + \alpha 2\pi\phi_0)}} \right].$$

Here, ϕ_0 is determined by the relation

$$\cos(2\pi\phi_0) = \cos\theta \cos(2\pi\phi), \quad (11)$$

and the matrix \hat{H} has the form

$$\hat{H} = \begin{pmatrix} a & b e^{i\xi} \\ b e^{-i\xi} & -a \end{pmatrix}, \quad (12)$$

where $\xi = \varphi - 2kx_0$, $k = \varepsilon/v_F$ is the electron momentum, and x_0 is the position of the MD, measured from the left contact. The coefficients

$$a = i \frac{e^{-2\pi i \phi} - \cos(2\pi\phi_0) \cos\theta}{\cos\theta \sin(2\pi\phi_0)}, \quad (13)$$

$$b = \frac{e^{-2\pi i \phi} \tan\theta}{\sin(2\pi\phi_0)}, \quad (14)$$

are related by the relation $a^2 + b^2 = 1$ and depend only on the strength of the defect and the magnetic flux. The energy dependence is present only in the off-diagonal terms of \hat{H} in exponents $e^{\pm i\xi}$.

4. COMPUTATION OF THE FF

We calculate the expression for the FF in the general case by substituting the matrix of transmission amplitudes (10) into the formula (6) and averaging over the energy in the limit $T \gg \Delta$. Technically, at such temperatures, energy averaging is reduced to calculating the integral $\langle \dots \rangle = \frac{L}{2\pi} \int_0^{2\pi/L} dk(\dots)$ [14, 15].

The analytical expression obtained after averaging is

rather cumbersome (a detailed derivation will be presented elsewhere) and we show it in the supplementary material. We will consider limiting cases to clarify the physical aspects of the problem.

4.1. HES without a MD

The simplest limiting case corresponds to the absence of a MD. In this case, the electron spin is conserved both during propagation along the ring and when entering or leaving a contact. There are no interference effects in this case since the spin is conserved, and different spins are described by orthogonal spinors. The transmission amplitude matrix in this case has a diagonal form,

$$\hat{t} = \begin{pmatrix} \frac{r^2 e^{ikL_1 + i2\pi\phi L_1/L}}{1 - t^2 e^{ikL + i2\pi\phi}} & 0 \\ 0 & \frac{r^2 e^{ikL_2 - i2\pi\phi L_2/L}}{1 - t^2 e^{ikL - i2\pi\phi}} \end{pmatrix}. \quad (15)$$

Expansion of the factors included in the diagonal terms $(1 - t^2 e^{ikL \pm i2\pi\phi})^{-1}$ in the Taylor series over t is the sum over the number of windings.

Using the expressions (3), (6), (15) and averaging over energy, we find that the FF does not depend on the magnetic flux and is related by a simple formula to the transmission coefficient:

$$\mathcal{F}[t, \theta = 0, \phi] = \frac{2t^2}{(1 + t^2)^2} = \frac{1 - \tilde{\mathcal{T}}^2}{2}. \quad (16)$$

Here, $\tilde{\mathcal{T}} = \langle \bar{\mathcal{T}} \rangle_\epsilon = (1 - t^2)/(1 + t^2)$. Equation (16) is shown by the blue line in Fig. 3.

4.2. Metal Contacts and Strong MD

Contact, in which an electron ideally tunnels into the HES, models a metallic contact. Accordingly, $r = 1$ and, as a consequence, $t = 0$ due to the unitarity of the contact scattering matrix. The last property means that the electron passes through the HES only from contact to contact, and there are no windings. If there is a strong MD in one of the arms, $\theta = \pi/2$, then the electron propagating in this arm is reflected from it and cannot reach the next contact. Thus, only electrons that move along the bottom edge of the sample (see Fig. 1) can pass through the interferometer. The transmission coefficients of such a system are given by $\mathcal{T}_\uparrow = \mathcal{R}_\downarrow = 0$ and $\mathcal{T}_\downarrow = \mathcal{R}_\uparrow = 1$. Therefore the shot noise is absent,

$$\mathcal{S} \propto (1 - \mathcal{T}_\uparrow)\mathcal{T}_\uparrow + (1 - \mathcal{T}_\downarrow)\mathcal{T}_\downarrow = 0, \quad (17)$$

because the passage of the electrons with spin ‘‘up’’ is completely blocked, while spin ‘‘down’’ passes through the edge of the sample without backscattering. Thus, a 2D TI with metal contacts, which has a strong MD at the edge, is a *noise-free ideal spin filter*.

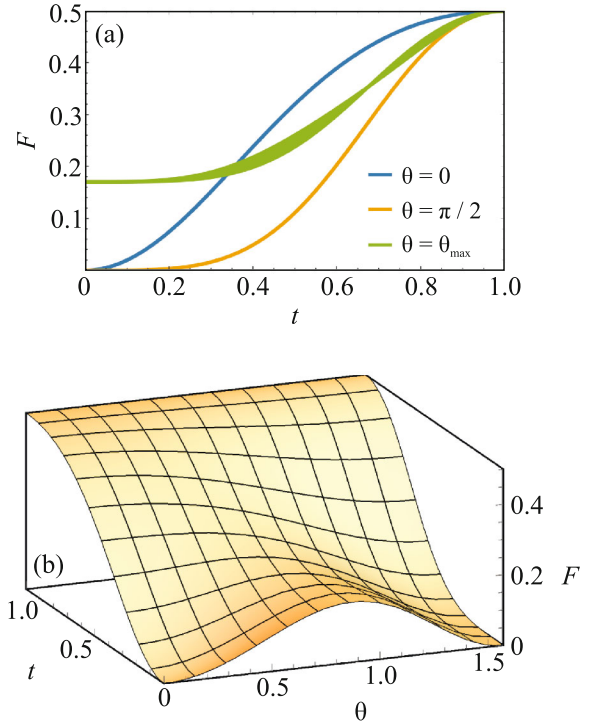


Fig. 3. (Color online) (a) The FF as a function of contact transparency, t , for different strength of the scattering on the MD, θ . The widened green curve shows the family of dependencies of \mathcal{F} on t for $\theta = \theta_{\max}$ and different ϕ . The width of this curve shows the change of \mathcal{F} with changing magnetic flux in the whole relevant interval: $0 < \phi < 1$. (b) Dependence of \mathcal{F} on t and θ for $\phi = 1/4$.

4.3. Strong MD and General Contacts

For the case of an arbitrary coupling strength with the contact, $0 < t < 1$, and strong MD, $\theta = \pi/2$, the matrix of transmission amplitudes is easily calculated by direct summation of the amplitudes and has the form

$$\hat{t} = \frac{r^2 e^{-i2\pi\phi L_2/L + ikL}}{1 + t^4 e^{2ikL}} \begin{pmatrix} -e^{ikL_1} t^2 & i e^{ik(L_1 - 2x_0)} t \\ i t e^{-ik(L_1 - 2x_0)} & e^{-ikL_1} \end{pmatrix}. \quad (18)$$

There is no magnetic flux in the denominator, because the passage through the HES with a non-zero number of windings includes only trajectories with a return to the MD, and there is an odd number of windings $2n + 1$, of which $n + 1$ turns clockwise, and n counterclockwise. An example of two processes without spin flip with 1 and 3 windings is shown in Fig. 4. The factor appears in the denominator $t^2 \exp[ikL + i2\pi\phi] t^2 \exp[ikL - i2\pi\phi] = t^4 \exp[2ikL]$ since each clockwise passage (except for one excess passage) is accompanied by a counterclockwise passage. In this case, the FF after averaging in the temperature window is still independent of the magnetic flux and has the following form:

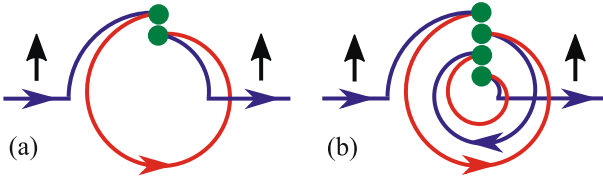


Fig. 4. (Color online) Processes without spin flipping after transmission of the interferometer with 1 (a) and 3 (b) windings for the case of a very strong defect.

$$\mathcal{F}[t, \theta = \pi/2, \phi] = \frac{2t^4}{(1+t^4)^2}. \quad (19)$$

This dependence is shown in Fig. 3 by the orange line.

4.4. Metallic Contacts and Magnetic Defect of Arbitrary Strength

We showed above that both in the absence of MD and for very strong MD, the FF becomes zero at $t = 0$, i.e., for a system with metallic contacts (see Eqs. (16) and (19), respectively).

Let us now consider the metallic contact with $t = 0$ and assume that the MD has an arbitrary strength, $0 < \theta < \pi/2$. In this case, the spins are completely separated and windings are absent. Therefore, the matrix of transmission amplitudes is calculated in a trivial way

$$\hat{t} = \begin{pmatrix} \cos \theta e^{ikL_1 + 2\pi\phi L_1/L} & 0 \\ 0 & e^{ikL_2 - 2\pi\phi L_2/L} \end{pmatrix}. \quad (20)$$

Accordingly, the FF has the form

$$\mathcal{F}[t = 0, \theta, \phi] = \frac{\sin^2 2\theta}{4(1 + \cos^2 \theta)}. \quad (21)$$

As θ increases from zero, \mathcal{F} increases, reaches a maximum, then decreases and again becomes zero in the limit of a very strong MD. Thus, there is an optimal value of the MD strength, which gives the maximum value of the FF, $\mathcal{F}_{\max} = 3 - 2\sqrt{2} \approx 0.17$. Physically, this case is equivalent to the case of two parallel channels—a completely ballistic one and a channel whose resistance is determined by scattering on the MD. The value of \mathcal{F}_{\max} is obtained by optimizing the expression $T_\theta(1 - T_\theta)/(1 + T_\theta)$ with respect to $T_\theta = \cos^2 \theta$.

4.5. General Case

Several simple limiting cases, analyzed above, contained no dependence on ϕ . However, a dependence on ϕ appears in a general case. General formula for $\mathcal{F}(t, \theta, \phi)$ is very cumbersome and we have provided it in the supplementary materials (see expressions (S.7)–(S.10) in the supplementary materials). This formula

clearly shows the dependence on ϕ . For example, for almost metallic contact, $t \ll 1$, for an arbitrary scattering strength on a MD, the FF shows weak oscillations with ϕ :

$$\begin{aligned} \mathcal{F}(t, \theta, \phi) \approx & \frac{R_\theta(1 - R_\theta)}{2 - R_\theta} + 2t^2 \\ & + 2t^4 \frac{R_\theta(1 - R_\theta)(10 - 12R_\theta + 3R_\theta^2)}{(2 - R_\theta)^2} \cos(4\pi\phi). \end{aligned} \quad (22)$$

Here, $R_\theta = 1 - T_\theta = \sin^2 \theta$ is the probability of back-scattering from a MD. More interesting is the opposite case of an almost tunnel contact: $t \rightarrow 1, r \ll 1$. In this case,

$$\mathcal{F}(t, \theta, \phi) \approx \frac{1}{2} - \frac{r^4}{8} - r^4 \frac{3R_\theta}{4((R_\theta - 1)\cos(4\pi\phi) + R_\theta + 1)}. \quad (23)$$

Although for the ideal tunnel contact, $r \equiv 0$, we obtain the universal value $\mathcal{F} = 1/2$, which corresponds to passing through localized independent levels in the system [40], dependence of \mathcal{F} on the flux appears when r deviates from unity. In particular, for the case of a weak defect, $R_\theta \ll 1$, FF shows sharp resonances of small amplitude around $\phi = 0$ and $\phi = 1/2$.

Note that the dependence of \mathcal{F} on the magnetic field turns out to be quite weak. Family of dependencies of the FF for the magnetic flux varying in the range from zero to unity at $\theta = \theta_{\max}$, i.e., $\mathcal{F}(\theta = \theta_{\max}, t, 0 < \phi < 1)$, is represented in Fig. 3 by the green broadened line. The width of this line shows the change in \mathcal{F} over the entire relevant range of magnetic flux variation: $0 < \phi < 1$. As can be seen, this width is significantly less than the distance between the two limiting curves corresponding to $\theta = 0$ and $\theta = \pi/2$. However, this dependence can be analyzed by studying the normalized value $\mathcal{F}_{\text{norm}}(t, \theta, \phi) = [\mathcal{F}(t, \theta, \phi) - \mathcal{F}(t, \theta, 1/4)]/[\mathcal{F}(t, \theta, 0) - \mathcal{F}(t, \theta, 1/4)]$. For example, from the formula (23) for $\theta \ll 1$ we obtain

$$\mathcal{F}_{\text{norm}} \approx \frac{\theta^2}{\theta^2 + \sin^2(2\pi\phi)},$$

i.e., sharp resonances at $\phi = 0$ and $\phi = 1/2$.

4.6. Comparison with a Conventional AB Interferometer

It is interesting to compare the obtained results with those for the shot noise of current through a conventional (non-helical) spinless single-channel AB interferometer. The calculation can be carried out completely similarly to the helical case (the conductance of such an interferometer was discussed in [41–43]). In this paper we will limit ourselves to the case of a ballistic conventional interferometer with identical arms. We provide formulas for this case in the supplementary materials (a more general case will be dis-

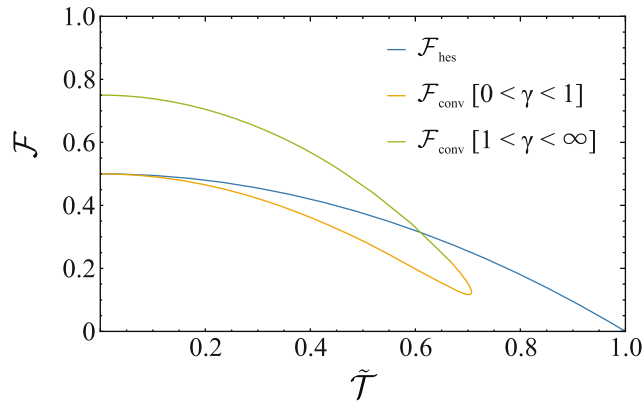


Fig. 5. (Color online) Dependence of the FF on the transmission coefficient of the interferometer: the blue curve is the helical interferometer without a MD when t changes in the range $0 < t < 1$ (described by the formula (16)); the orange and green curve correspond to a single-channel conventional (non-helical) interferometer at $\phi = 0.25$ and changing the tunneling parameter γ in the range $0 < \gamma < 1$ and $1 < \gamma < \infty$, respectively (see supplementary materials). At $\phi = 0$ the orange and green curves “merge” and coincide with the blue curve.

cussed elsewhere). At $\phi = 0$, the dependence of the FF on the conductance is given by the same formula for the helical and the conventional interferometers (see Eqs. (16) and (S.11)). However, in the conventional interferometer, dependence on ϕ occurs even without impurities due to the possibility of backscattering at the contacts. Therefore, at $\phi \neq 0$ the dependencies cease to coincide, as illustrated in Fig. 5. Two different branches of the dependence $\mathcal{F}(\tilde{T})$ arise due to the fact that in a conventional interferometer the same conductance can be realized by contacts of different types (see panels (a) and (b) of the Fig. S1 in the supplementary materials). The most striking difference occurs at $\phi = 1/2$. In this case, in the conventional AB interferometer, there is exact destructive interference for any energy, i.e., the transmission amplitude is identically zero at all energies, $t(\epsilon, \phi = 1/2) \equiv 0$ [38] (see also the discussion of the consequences of this identity in [41, 42]). As a result, in a conventional interferometer $\mathcal{F} \rightarrow 1$ for $\delta\phi = \phi - 1/2 \rightarrow 0$ (see Eqs. (S.5) and (S.7) from the supplementary materials and discussion there).

5. CONCLUSIONS

Important conclusions and predictions for possible experiments can be made by analyzing Fig. 3. One can see that for a metallic contact ($t \rightarrow 0$), the introduction of a MD significantly increases the noise. For tunnel contacts with very weak tunnel coupling ($t \rightarrow 1$), the dependence on the strength of the defect

is weak and, moreover, in a contrast to metallic contact, the MD slightly reduces the FF.

To summarize, we have obtained an expression for the FF of current flowing along the edge of a 2D TI with a MD in two-terminal geometry. The obtained expression was analyzed in different limiting cases depending on the strength of scattering by the MD and the transparency of the contacts. The dependence of \mathcal{F} on the magnetic field has also been studied.

SUPPLEMENTARY INFORMATION

The online version contains supplementary material available at <https://doi.org/10.1134/S0021364024600186>.

ACKNOWLEDGMENTS

We are grateful to I.S. Burmistrov for fruitful discussions.

FUNDING

This work was supported by the Russian Science Foundation (project no. 20-12-00147-P, D.N. Aristov, V.Yu. Kachorovskii), by the Council of the President of the Russian Federation for State Support of Young Russian Scientists and Leading Scientific Schools (project no. MK-2918.2022.1.2, R.A. Niyazov, calculation of the Fano factor in the general case, Section 4.5 and the supplementary materials), and in part by the Foundation for the Advancement of Theoretical Physics and Mathematics BASIS (R.A. Niyazov).

CONFLICT OF INTEREST

The authors of this work declare that they have no conflicts of interest.

OPEN ACCESS

This article is licensed under a Creative Commons Attribution 4.0 International License, which permits use, sharing, adaptation, distribution and reproduction in any medium or format, as long as you give appropriate credit to the original author(s) and the source, provide a link to the Creative Commons license, and indicate if changes were made. The images or other third party material in this article are included in the article’s Creative Commons license, unless indicated otherwise in a credit line to the material. If material is not included in the article’s Creative Commons license and your intended use is not permitted by statutory regulation or exceeds the permitted use, you will need to obtain permission directly from the copyright holder. To view a copy of this license, visit <http://creativecommons.org/licenses/by/4.0/>

REFERENCES

1. B. Bernevig and T. Hughes, *Topological Insulators and Topological Superconductors* (Princeton Univ. Press, Princeton, 2013).
2. M. Z. Hasan and C. L. Kane, *Rev. Mod. Phys.* **82**, 3045 (2010).
3. X.-L. Qi and S.-C. Zhang, *Rev. Mod. Phys.* **83**, 1057 (2011).
4. C. L. Kane and E. J. Mele, *Phys. Rev. Lett.* **95**, 226801 (2005).
5. B. A. Bernevig, T. L. Hughes, and S. C. Zhang, *Science* (Washington, DC, U. S.) **314**, 1757 (2006).
6. M. König, S. Wiedmann, C. Brune, A. Roth, H. Buhmann, L. W. Molenkamp, X.-L. Qi, and S.-C. Zhang, *Science* (Washington, DC, U. S.) **318**, 766 (2007).
7. A. Roth, C. Brüne, H. Buhmann, L. W. Molenkamp, J. Maciejko, X.-L. Qi, and S.-C. Zhang, *Science* (Washington, DC, U. S.) **325**, 294 (2009).
8. G. M. Gusev, Z. D. Kvon, O. A. Shegai, N. N. Mikhailov, S. A. Dvoretzky, and J. C. Portal, *Phys. Rev. B* **84**, 121302 (2011).
9. C. Brüne, A. Roth, H. Buhmann, E. M. Hankiewicz, L. W. Molenkamp, J. Maciejko, X.-L. Qi, and S.-C. Zhang, *Nat. Phys.* **8**, 485 (2012).
10. A. Kononov, S. V. Egorov, Z. D. Kvon, N. N. Mikhailov, S. A. Dvoretzky, and E. V. Deviatov, *JETP Lett.* **101**, 814 (2015).
11. P. Delplace, J. Li, and M. Büttiker, *Phys. Rev. Lett.* **109**, 246803 (2012).
12. F. Dolcini, *Phys. Rev. B* **83**, 165304 (2011).
13. G. Gusev, Z. Kvon, O. Shegai, N. Mikhailov, and S. Dvoretzky, *Solid State Commun.* **205**, 4 (2015).
14. R. A. Niyazov, D. N. Aristov, and V. Y. Kachorovskii, *Phys. Rev. B* **98**, 045418 (2018).
15. R. A. Niyazov, D. N. Aristov, and V. Y. Kachorovskii, *npj Comput. Mater.* **6** (2020).
16. R. A. Niyazov, D. N. Aristov, and V. Y. Kachorovskii, *Phys. Rev. B* **103**, 125428 (2021).
17. R. A. Niyazov, D. N. Aristov, and V. Y. Kachorovskii, *JETP Lett.* **113**, 689 (2021).
18. R. A. Niyazov, D. N. Aristov, and V. Y. Kachorovskii, *Phys. Rev. B* **108**, 075424 (2023).
19. R. A. Niyazov, D. N. Aristov, and V. Y. Kachorovskii, *JETP Lett.* **118**, 376 (2023).
20. N. Lezmy, Y. Oreg, and M. Berkooz, *Phys. Rev. B* **85**, 235304 (2012).
21. A. Del Maestro, T. Hyart, and B. Rosenow, *Phys. Rev. B* **87**, 165440 (2013).
22. J. M. Edge, J. Li, P. Delplace, and M. Büttiker, *Phys. Rev. Lett.* **110**, 246601 (2013).
23. F. Dolcini, *Phys. Rev. B* **92**, 155421 (2015).
24. E. S. Tikhonov, D. V. Shovkun, V. S. Khrapai, Z. D. Kvon, N. N. Mikhailov, and S. A. Dvoretzky, *JETP Lett.* **101**, 708 (2015).
25. J. I. Väyrynen and L. I. Glazman, *Phys. Rev. Lett.* **118**, 106802 (2017).
26. S. U. Piatrusha, L. V. Ginzburg, E. S. Tikhonov, D. V. Shovkun, G. Koblmüller, A. V. Bubis, A. K. Grebenko, A. G. Nasibulin, and V. S. Khrapai, *JETP Lett.* **108**, 71 (2018).
27. K. E. Nagaev, S. V. Remizov, and D. S. Shapiro, *JETP Lett.* **108**, 664 (2018).
28. P. D. Kurilovich, V. D. Kurilovich, I. S. Burmistrov, Y. Gefen, and M. Goldstein, *Phys. Rev. Lett.* **123**, 056803 (2019).
29. V. D. Kurilovich, P. D. Kurilovich, I. S. Burmistrov, and M. Goldstein, *Phys. Rev. B* **99**, 085407 (2019).
30. B. V. Pashinsky, M. Goldstein, and I. S. Burmistrov, *Phys. Rev. B* **102**, 125309 (2020).
31. C.-H. Hsu, P. Stano, J. Klinovaja, and D. Loss, *Semicond. Sci. Technol.* **36**, 123003 (2021).
32. B. Probst, P. Virtanen, and P. Recher, *Phys. Rev. B* **106**, 085406 (2022).
33. S. Munyan, A. Rashidi, A. C. Lygo, R. Kealhofer, and S. Stemmer, *Nano Lett.* **23**, 5648 (2023).
34. D. V. Khomitsky, A. A. Konakov, and E. A. Lavrukhiina, *J. Phys.: Condens. Matter* **34**, 405302 (2022).
35. V. A. Sablikov and A. A. Sukhanov, *Phys. Rev. B* **103**, 155424 (2021).
36. P. P. Aseev and K. E. Nagaev, *Phys. Rev. B* **94**, 045425 (2016).
37. E. Olshanetsky, G. Gusev, A. Levin, Z. Kvon, and N. Mikhailov, *Phys. Rev. Lett.* **131**, 076301 (2023).
38. M. Büttiker, Y. Imry, and M. Y. Azbel, *Phys. Rev. A* **30**, 1982 (1984).
39. M. J. M. de Jong and C. W. J. Beenakker, in *Mesoscopic Electron Transport*, Ed. by L. Sohn, L. Kouwenhoven, and G. Schön, Vol. 345 of *NATO ASI Series E* (Kluwer Academic, Dordrecht, 1997), p. 225.
40. Y. Blanter and M. Büttiker, *Phys. Rep.* **336**, 1 (2000).
41. A. P. Dmitriev, I. V. Gornyi, V. Y. Kachorovskii, and D. G. Polyakov, *Phys. Rev. Lett.* **105**, 036402 (2010).
42. A. P. Dmitriev, I. V. Gornyi, V. Y. Kachorovskii, D. G. Polyakov, and P. M. Shmakov, *JETP Lett.* **100**, 839 (2015).
43. A. P. Dmitriev, I. V. Gornyi, V. Y. Kachorovskii, and D. G. Polyakov, *Phys. Rev. B* **96**, 115417 (2017).

Publisher's Note. Pleiades Publishing remains neutral with regard to jurisdictional claims in published maps and institutional affiliations.